Heating Treatment as a Simple Approach to Improve Lignin Filtration Efficiency in the LignoBoost Process

ACS Sustainable Chemistry & Engineering

pubs.acs.org/journal/ascecg

Research Article

Heating Treatment as a Simple Approach to Improve Lignin Filtration Efficiency in the LignoBoost Process

Hampus Johansson, Liam Mistry, Ahilan Manisekaran, Henrik Sarge, Anette Larsson, Li-Yang Liu,* Merima Hasani, and Hans Theliander

Cite This: https://doi.org/10.1021/acssuschemeng.5c12647

Read Online

ACCESS | Metrics & More | Article Recommendations | Supporting Information

ABSTRACT: The LignoBoost process enables efficient isolation of high-purity lignin from black liquor; however, lignin colloidal behavior during the acidic washing step strongly influences the filtration performance, and the impacts of temperature remain insufficiently understood. In this study, Kraft lignin suspensions were thermally treated at 75 °C, 85 °C, and 95 °C to evaluate their effects on volumetric flow rate during filtration and on lignin physicochemical properties. Thermal treatment at 85 °C yields the optimal filtration efficiency, with the volumetric flow rate increasing by 11-fold (lignin A) and 19-fold (Lignin B) compared to the control group. Particle size analysis revealed clear lignin particle growth after heating treatment, which was accompanied by a decrease in smaller particles. Beyond physical noncovalent interactions, chemical contributions to particle growth were elucidated by analyzing radical concentration, molar mass, and structural features. Radical concentrations decreased significantly, accompanied by increased condensation and reduced ester linkages in the recovered lignin. The molar mass changed slightly. Despite these changes, the overall functional group content (methoxy, aliphatic hydroxyl groups, and aromatic hydroxyl groups) and glass transition temperature remained largely unchanged. This work elucidates the interactive effects of heating treatment on lignin structure and recovery performance, providing a mechanistic understanding to optimize kraft lignin separation and thereby promote its subsequent valorization.

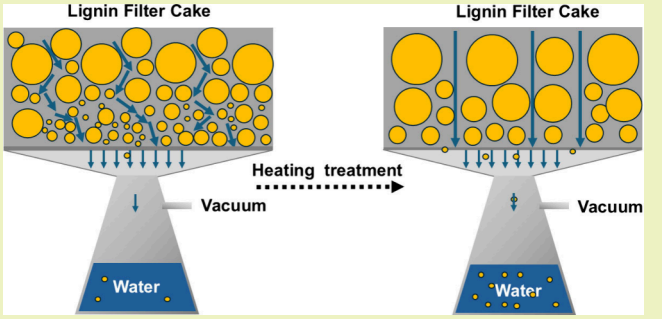

KEYWORDS: *Kraft lignin, Heating treatment, LignoBoost, Filter cake, and Filtration efficiency*

1. INTRODUCTION

Annually, more than 70 million metric tons of kraft lignin have been efficiently extracted as a side product from the chemical pulp industry.[1] The woody biomass is delignified with sodium hydroxide and sodium sulfide (white liquor), producing cellulose pulp and black liquor; the latter, which contains kraft lignin, salts, sugar, sugar derivatives, and extractives, is usually concentrated and incinerated for power generation and salt recycling.[2] However, increasing environmental and economic pressures have driven the pulp industry to convert these underutilized resources into materials and chemicals to meet our growing demand for renewable resources.[3] The transition toward the biorefinery process will improve their carbon footprint and economic efficiency.[4] Recently, Kraft lignin has demonstrated outstanding potential for making advanced materials, such as polyurethane foams,[5] wood coatings,[6] aerogels for supercapacitors,[7] carbon fibers,[8] etc. Modified kraft lignin as an additive can efficiently toughen thermoplastics, including poly(ethylene terephthalate),[9] and poly(butylene adipate terephthalate).[10] Functionalized lignin with fatty acids can enhance pesticide delivery to the leaf surface, thereby assisting plant growth.[11] Most of this valorization require dried lignin powders with desired performance, including, but not limited to, high consistency, high purity (low sugar and ash content), high yield, good solubility in a benign organic solvent, versatile reactivity, and a uniform molecular weight distribution.[3]

As such, the recovery and purification of lignin from black liquor are crucial for satisfying these requirements. Industry and academia have been investigating this process for decades.[1] Dating back to the 1940s, Tomlinson patented the earliest lignin recovery process that used CO_2 and sulfuric acid as acidic agents to precipitate the lignin.[12] For many years, Westvaco Company (now Ingevity Corp.) in North Carolina (US) has been the only commercial provider of Kraft lignin, which is trademarked as Indulin AT.[13] In 1996, STFI Innventia AB and Chalmers University of Technology in Sweden began a

Received: November 27, 2025
Revised: January 28, 2026
Accepted: January 29, 2026

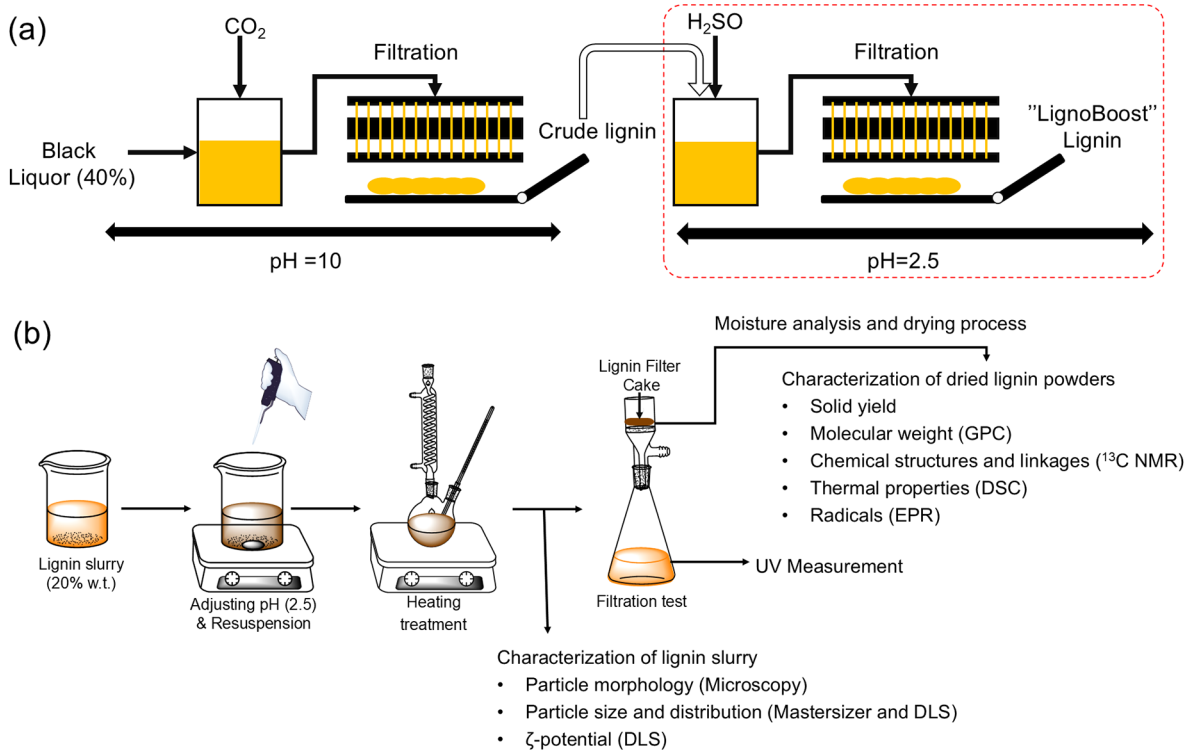

Figure 1. Experimental setup for the LignoBoost Process, including a two-step acidification and filtration process (a); the laboratory setup on the heating treatment process and characterization methodologies involved (b).

collaborative project to advance lignin recovery based on Tomlinson's process and this isolation process was named LignoBoost, now owned by Valmet.[14] In 2013, Domtar adopted this process to isolate the softwood kraft lignin BioChoice (now owned by UPM). Chang and collaborators compared BioChoice with Indulin AT, showing that these two lignins (both from pine) are similar in chemical structure and molecular weight, but BioChoice lignin from the LignoBoost process has a lower ash content and better solvent solubility. Moreover, the process offers advantages that address problems such as filter clogging, low lignin yield, low consistency, and adverse effects on salt balances.[15] Valmet has commercialized this process and has been adopted by multiple pulping companies: Domtar (2013, Plymouth, US), Stora Enso (2015, Finland), Klabin (2019, Brazil), and Mercer International (2023, Germany).

Specifically, Lignoboost comprises two washing steps: a high-pH step and a low-pH step. Black liquor (30−40 wt %) is first blown with CO_2 to decrease its pH (from 14 to about 9). The pH change in the black liquor with subsequent heat treatment can lead to the formation of larger lignin particles. This crude lignin can be filtered efficiently under additional mechanical pressure, such as pressurized chamber filter (Figure 1a). To improve purity, crude lignin is loaded into a tank and resuspended in aqueous sulfuric acid (around pH 2) at a 20% concentration with continuous stirring. This method reduces the use of washing agents and improves washing efficiency compared to traditional water-displacement filtration.[16] However, the resuspension of lignin particles can lead to the formation of lignin colloids, which can negatively affect filtration resistance during vacuum belt filtration. Researchers at Valmet recently found that applying a thermal treatment to the lignin suspension prior to filtration can effectively tailor its filtration properties and improve the process performance.[17] According to the Derjaguin−Landau−Verwey−Overbeek (DLVO) theory, pH, composition, temperature, and ionic strength can all affect lignin colloidal behavior.[18] Ionic strength, pH, and composition have been investigated in previous studies.[19]

In this study, we aim to elucidate the impact of the temperature alone on the filtration efficiency of a lignin suspension during the low-pH washing step. Two sets of kraft lignins A and B are used. These lignins are obtained from two different pulp mills (Stora Enso) and isolated from the LignoBoost process. The wet lignin suspension was redispersed in acidic water at 55 °C (control) and then thermally treated at 75 °C, 85 °C, and 95 °C. The filtration efficiency was evaluated based on the volumetric flow rate (dV/dt). We hypothesize that both physical and chemical mechanisms play crucial roles in changing the lignin size and in influencing subsequent filtration efficiency. The particle size in the lignin suspension was thoroughly characterized by optical microscopy, Mastersizer, and dynamic light scattering (DLS), as shown in Figure 1b. Their chemical structures are also quantified to determine the radical concentration (electron paramagnetic resonance), molar mass (gel permeation chromatography), T_g (glass transition temperature), and chemical structure (quantitative ^{13}C nuclear magnetic resonance). This work provides critical insight into how lignin isolation processes shape lignin structure and, in turn, its filtration performance. By establishing clear links between processing and structure, our findings offer an important foundation for the large-scale valorization of kraft lignin in high-value applications.

https://doi.org/10.1021/acssuschemeng.5c12647
ACS Sustainable Chem. Eng. XXXX, XXX, XXX−XXX

2. MATERIALS AND METHODS

2.1. Lignin Resources and Chemicals

Lignin A and lignin B were kindly provided by Stora Enso and were received as solid powders. Their moisture contents are 58.1 wt % (A) and 36.8 wt % (B), respectively, measured in triplicate using a moisture analyzer (Sartorius MA 30, Germany). They were extracted from softwood black liquor after the kraft pulp process and recovered after the low-pH step (Figure 1a). Acetic anhydride (ACS reagent), pyridine (99%), dimethyl sulfoxide (ACS reagent), and deuterium dimethyl sulfoxide (DMSO-d6) were all purchased from Sigma-Aldrich. Concentrated sulfuric acid (98% H_2SO_4) was purchased from Fischer Scientific.

2.2. Lignin Slurry Preparation, Heating Treatment, and Filtration

The preparation of lignin slurry is like the industrial-scale LignoBoost process, as shown in Figure 1. Lignin A and lignin B suspensions were prepared by dispersing lignin powders in acidic deionized water at pH 2.5 to ensure the final suspensions consisted of 20% lignin by weight percentage. The total volume for lignin B is 20% lower than that of the lignin A suspension. After that, the pH was further adjusted to exactly 2.5 with concentrated sulfuric acid (H_2SO_4), and the mixture was stirred for another 60 min at 55 °C.

Heating treatment is performed by transferring the lignin suspensions (A and B) into a 500 mL round-bottom flask with a condenser and a thermometer. The flask is loaded into an oil bath with a magnetic stirrer. Suspension was first stabilized at 55 °C for 60 min with continuous stirring (control group), then heated to 75 °C, 85 °C, or 95 °C for 60 min. Five ml of treated lignin slurry was then taken and stored in 4 °C refrigerator. Later, the lignin slurry is characterized using a Mastersizer, optical microscopy, and a zeta-sizer.

Filtration efficiency is evaluated based on the volumetric flow rate of the lignin cake. The treated and untreated lignin suspensions were cooled to 60 °C (except for the control group) in a water bath and then poured onto a vacuum filter. The filter paper is made from ashless cellulose (Munktell Filtra, Sweden) with a 70 mm diameter and particle retention (1−2.5 μm). The filtration time (t) was recorded based on experimental observation and results. Specifically, when the top of the filter cake appeared less moist and the supernatant dripping stopped, the vacuum promptly ceased to record the filtration time (t). The filter cake was removed from the vacuum filter. Their moisture contents (X) were measured by using the moisture analyzer. The volumetric flow rate is calculated as $dV/dt = (80\% - X)/t$. Lignin filter cakes were dried in a vacuum oven at 50 °C overnight before subsequent characterization. The solid yield is measured by weighing the dried lignin (W). The supernatant is characterized by UV−vis spectroscopy (Specord 205, Analytik Jena) from 700 to 210 nm to identify components in the liquor. (Supplementary Figure 1b) Three replicates were performed for lignin A at each treatment temperature, whereas only one replicate for lignin B was tested due to limited material supply.

2.3. Characterization of Lignin Slurry

2.3.1. Optical Microscopy Analysis. A 20 μL aliquot of lignin slurry after thoroughly shaking was diluted with 2 mL of acidic deionized water (pH 2−4). A total of 20 μL of the diluted sample was mounted on a glass slide for optical analysis with a Zeiss Discovery V.12, using a Zeiss KL1500 LCD as the light source. The magnification used was 230× for all samples.

2.3.2. Mastersizer Analysis. A Mastersizer 2000 with a Hydro 2000 module (Malvern Panalytical, Netherlands) was used to analyze particle size. Samples were extracted directly from lignin suspension during heat treatment and mixed with acidic deionized water (pH = 2−4). The samples were then placed into the Hydro 2000s until the laser obstruction reached between 9% and 10%. The mixer rotating speed was set to 1750 rpm, while the ultrasound intensity was adjusted to 100%. Additionally, the refractive index of lignin was determined to be 1.61. All measurements were performed in triplicate to ensure reproducibility, and the spectra were corrected to a common baseline for comparison.

2.3.3. Dynamic Light Scattering Analysis. The particle size and ζ (zeta) potential of lignin suspensions subjected to different heat treatments were characterized by using a Malvern Zetasizer Ultra. The detailed preparation method is described in the previous paper.[20] Briefly, 0.2 mL of a lignin suspension was mixed with 1.8 mL of Milli-Q water. All samples were uniformly diluted 10-fold and thoroughly vortexed before measurements to ensure comparability. Disposable cuvettes and Folded Capillary Zeta Cells (DTS1070) were utilized for the size and ζ-potential measurements, respectively. All samples were measured in triplicate, with 12−15 runs of measurements per repetition.[20]

2.4. Characterization of Dried Lignin Powders

2.4.1. Differential Scanning Calorimetry Analysis. Differential scanning calorimetry (DSC) was performed to provide complementary information about the thermal properties of lignin. Samples were weighed between 2 and 5 mg in a hermetic aluminum sample pan. The DSC had an N2 gas flow of 50 mL/min. The temperature started at 25 °C, increased to 200 °C, and then decreased to 0 °C at a rate of 10 °C/min. This cycle was repeated once more. The DSC instrument utilized was a Mettler Toledo DSC5+.[21]

2.4.2. Electron Paramagnetic Resonance Spectroscopy. A total of 20 mg of thermal-treated lignin powders were transferred into a quartz EPR tube (O.D. 4.0 mm), sealed to prevent contamination or moisture ingress, and positioned at the center of the resonator for optimal signal detection. EPR measurements were conducted using a Linev SpinScan-X spectrometer operating at a microwave frequency of approximately 9.46 GHz (X-band). Operation and data collection was achieved using eSpinoza (version 1.1.0.2), published by Linev Systems. Modulation of the magnetic field was set at a frequency of 100 kHz, with a modulation amplitude (100−200 μT) adjusted to optimize signal resolution without overmodulating the spectrum. Spectra were recorded at 294 K. The magnetic field was swept over the 300 to 380 mT range, with a sweep time of 240 s. The microwave power was measured at intervals between 5 and 25 dB to avoid saturation effects while maintaining a sufficient signal intensity.

2.4.3. Gel Permeation Chromatography. A total of 10 mg of dried lignin sample was dissolved in 1 mL of DMSO containing 10 mM LiBr and filtered through a syringe filter (0.45 μm PTFE). The GPC instrument was a PL-GPC 50 from Polymer Laboratories. The instrument consists of an autosampler, pump, and fractionation columns, including a guard column and two 300 × 7.5 mm PolarGel-M columns. The eluent is DMSO containing 0.5 wt % LiBr with a temperature of 50 °C and a 0.5 mL/min flow rate. The fractionated lignin was analyzed with an ultraviolet (UV) detector. Pullulan standards (180 Da, 667 Da, 5900 Da, 11100 Da, 21100 Da, 47100 Da, 107 000 Da, 200 000 Da, 375 000 Da, and 708 000 Da) were analyzed to prepare the standard curves for conventional calibration analysis.[22]

2.4.4. Nuclear Magnetic Resonance Analysis. Samples for ^{13}C NMR were prepared by dissolving 150 mg of lignin in 500 μL of DMSO-d6 (Sigma-Aldrich), followed by the addition of 3 mg of Cr(III) acetylacetonate as a relaxation agent. Acetylated lignin samples were also prepared following our previous procedures.[23] ^{13}C NMR spectra were recorded using NMR facilities (800 MHz, Bruker) with a cryoprobe using parameters: pulse program zgzrse.2, number of scans 64, acquisition time 0.52 s, and delay time 5 s.

3. RESULTS AND DISCUSSION

3.1. Effects of the Heating Process on the Volumetric Flow Rate

Filtration efficiency is critical in the LignoBoost process and can be quantitatively assessed by measuring the volumetric flow rate of the lignin suspension (dV/dt). (Figure 2) The dV/dt for lignin A (control) is 2.6 mL/min, significantly lower than that of lignin B (control), which is 31.8 mL/min. This can be attributed to differences in their components (e.g., high-sugar

https://doi.org/10.1021/acssuschemeng.5c12647
ACS Sustainable Chem. Eng. XXXX, XXX, XXX−XXX

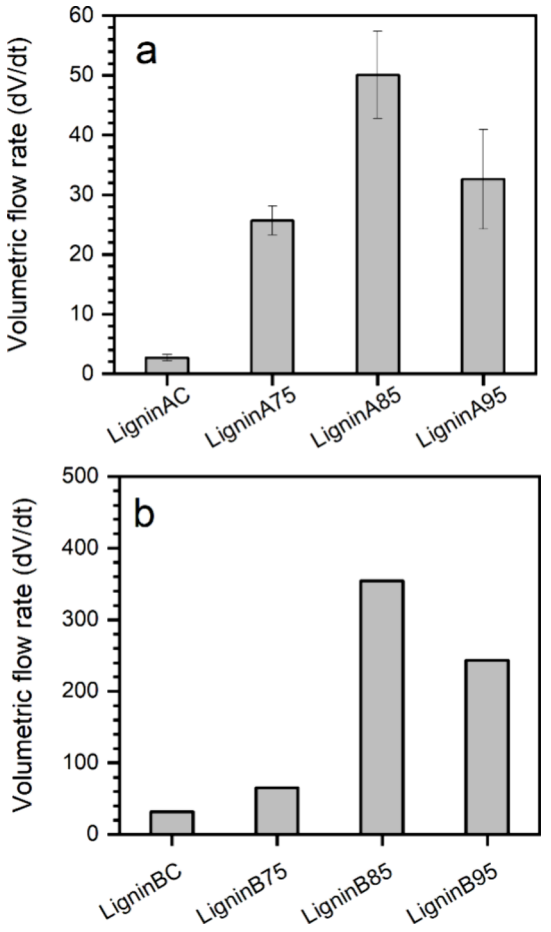

Figure 2. Heating temperature effects on volumetric flow rate (dv/dt) for lignin suspension A (a) and lignin suspension B (b).

components) or isolation conditions (e.g., pulping conditions), which may yield lignin particles with distinct properties (size and shape). It requires investigation in the future. Heating lignin suspensions before filtration can increase dV/dt by 9.8-fold (lignin A, 75 °C), 19.0-fold (lignin A, 85 °C), and 12.0-fold (lignin A, 95 °C) (Figure 2a). A similar trend also applied to lignin B suspensions (Figure 2b). This phenomenon has been verified at an industrial-scale LignoBoost process, but the effects of the thermal treatment temperature on dV/dt remain poorly understood. This is the primary objective of this study.[24]

This study controls the effective concentration (c), filtration area (A), and pressure control (ΔP) under the same conditions (eq 1). Water solvent filtered at the same temperature can be treated as the same eluent with a similar viscosity. As such, the specific resistance of the filter cake (α) is dependent on the effect of particle size (χ), lignin density (ρ_s), and porosity (ε), as described in eq 2. Porosity is a function of the particle size distribution and particle shape. Ideally, the filter cake, consisting of particles with a round, large, and homogeneous distribution, has the highest volumetric filtration rate. A wide-size distribution can be packed more tightly, significantly inhibiting the volumetric flow.

$$\frac{dV}{dt} = \frac{A\Delta p}{\mu(\alpha C v + AR)} \quad (1)$$

$$\alpha = \frac{180}{\rho_s \chi^2} \times \frac{1-\varepsilon}{\varepsilon^3} \quad (2)$$

Increasing the temperature markedly reduces the solid yield, dropping from 97.7% in the lignin A-control to 91.5% at 75 °C, 86.7% at 85 °C, and 81.3% at 95 °C (Supplementary Figure 1a). UV−vis spectroscopy analysis of the filtrate (Supplementary Figure 1b) shows an inverse trend: higher heating temperatures result in greater lignin loss in the filter cake. This phenomenon can be attributed to a less densely packed lignin cake with increased porosity (eq 2), which facilitates the passage of smaller lignin particles through the filter cake and filter paper. In some cases, smaller particles may obstruct the filter paper, explaining the observed decrease in dV/dt as the lignin suspension approaches 95 °C.

3.2. Effects of the Heating Process on the Lignin Particle Morphology

The lignin cake porosity is mainly controlled by particle size and distribution, which are thoroughly characterized using optical microscopy, a Mastersizer, and dynamic light scattering. The optical microscopy images show that the lignin particle size (control) is less than 50 μm. (Figure 3a,e) Most large particles have irregular shapes; their number is much less than

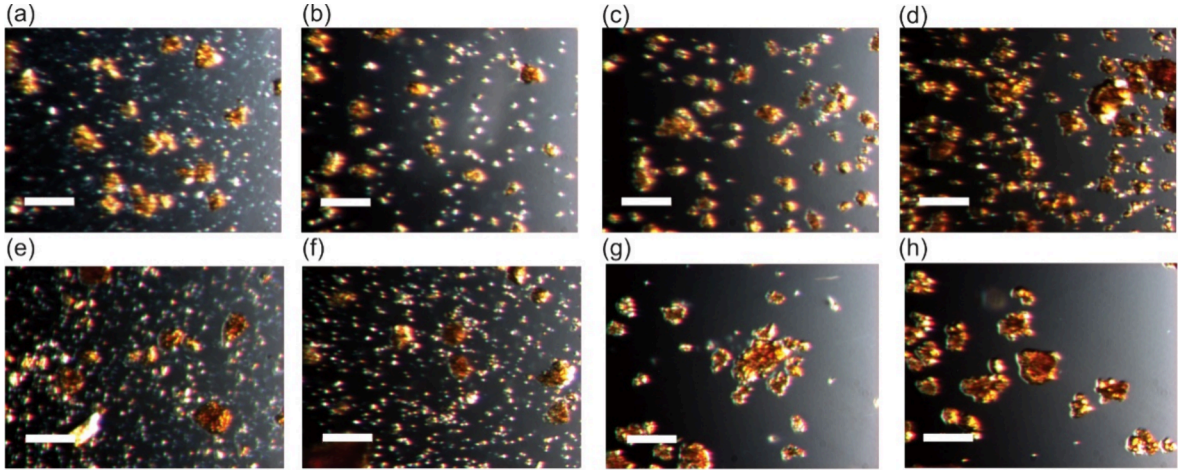

Figure 3. Optical microscopy of lignin suspension A (a, b, c, and d) and lignin suspension B (e, f, g, and h), including the control group (a, e) and samples thermally treated at 75 °C (b, f), 85 °C (c, g), and 95 °C (d, h); the scale bar is 50 μm.

https://doi.org/10.1021/acssuschemeng.5c12647
ACS Sustainable Chem. Eng. XXXX, XXX, XXX−XXX

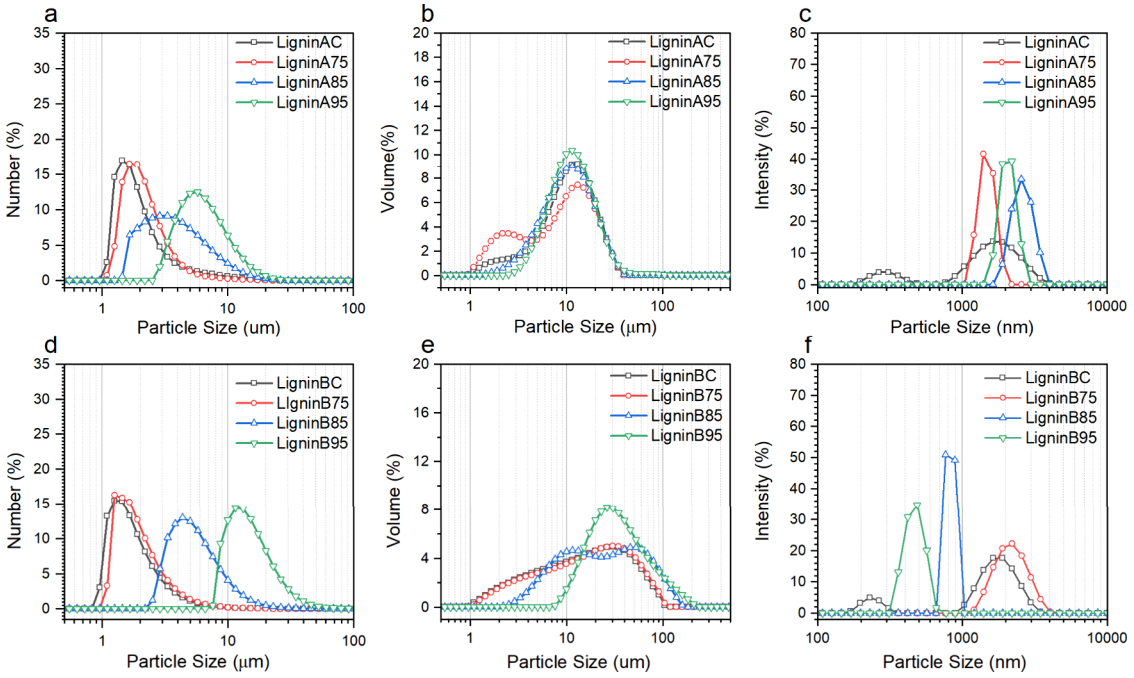

Figure 4. Particle size distribution curve of lignin suspension A (top) and lignin suspension B (bottom), including number- and volume-weighted distributions measured by Mastersizer (a, b, d, e) and particle size distribution curve determined by dynamic light scattering (c, f).

that of smaller-sized lignin particles. After heat treatment, the number of smaller lignin particles decreases significantly, accompanied by the formation of larger lignin particle clusters. The magnitude of this effect increases with temperature, being most evident at 95 °C (Figure 3d,h), followed by 85 °C (Figure 3c,g) and 75 °C (Figure 3b,f). Lignin A (Figure 3, top) and lignin B (Figure 3, bottom) showed similar trends. We can conclude that heating treatment may lead to lignin aggregation and particle growth, especially in smaller lignin particles, which have larger surface areas and enhanced reactivity.

3.3. Effects of the Heating Process on the Lignin Particle Size and Distribution

The Mastersizer and dynamic light scattering (DLS) are employed to analyze the entire particle size distribution of the lignin suspension (Figure 4). The Mastersizer determines particle size distribution from 0.01 to 3500 μm via light diffraction based on Mie scattering theory. The number weighted diameter (D_n, Supplementary Table 1) and number weighted diameter (D_v, Supplementary Table 2) are measured. However, the presence of large lignin particles (>1 μm) can interfere with the light diffraction signal from smaller particles, leading to an underestimation of their abundance. To address this, DLS was used to analyze smaller particles using a different mechanism based on Brownian motion. Before the measurement, we allow the larger particles to sediment naturally under gravity in the cuvettes, which more closely approximates the actual situation (Supplementary Figure 2). As the initial concentration is unclear, the ζ-potential (Supplementary Figure 3) and particle size (Figure 4c,f) are evaluated qualitatively rather than quantitatively in this study.

According to Mastersizer analysis (Figure 4a,b,d,e), the control groups for lignins A and B exhibit similar particle sizes and heterogeneous distribution curves ranging from 1 to 10 μm. Thermal treatment causes a rightward shift, significantly decreasing the number of smaller particles and increasing the number of larger ones. The number-based median particle size (D_n50) increases with temperature, from 1.65 μm (control A) and 1.49 μm (control B) to 1.87 μm (A) and 1.65 μm (B) at 75 °C, then to 3.33 μm (A) and 4.76 μm (B) at 85 °C, and finally to 5.66 μm (A) and 13.05 μm (B) at 95 °C (Supplementary Table 1). The volume-based median particle size (D_v50) shows similar trends, especially for lignin B—rising from 14.85 μm (control) to 15.97 μm at 75 °C, 21.41 μm at 85 °C, and 29.84 μm at 95 °C. The volume-weighted particle size distribution (PSD) decreases from 1.65 (control A) and 3.13 (control B) to 1.44 (A) and 2.26 (B) at 95 °C. For lignin A, the D_v50 change is less pronounced, but D_v10—the maximum particle diameter below which 10% of the sample volume exists—increases significantly from 3.83 μm (control) to 4.78 μm at 85 °C and 6.11 μm at 95 °C (Supplementary Table 2). That means smaller particles have been changed more obviously. Notably, thermal treatment at 75 °C markedly increases the volumetric flow rate compared with the control, even though the particle size and particle size distribution (PSD) remained largely unchanged (Figure 4 and Supplementary Figure 2). In contrast, lignin treated at 95 °C (groups A and B) exhibits significantly larger particle sizes and a narrower PSD, which would theoretically result in a higher cake porosity and thus a higher volumetric flow rate. However, the measured dV/dt at 95 °C is lower than that observed at 85 °C. This seemingly unexpected behavior suggests that factors beyond the particle analyzed range by laser diffraction may be important, particularly the presence of smaller particles, which have been underestimated by Mastersizer.

To investigate these smaller particles, we employed dynamic light scattering (DLS). DLS results show that particles smaller than 0.5 μm are absent in lignin treated at 75 °C (lignin A), whereas such small particles are clearly present in the control samples for both lignins A and B (Figure 4b,e). A further comparison between the 85 and 95 °C treatments reveals pronounced differences in the submicrometer particle fraction. Lignin treated at 95 °C contains a higher proportion of even

https://doi.org/10.1021/acssuschemeng.5c12647
ACS Sustainable Chem. Eng. XXXX, XXX, XXX−XXX

smaller particles, likely because elevated temperatures disrupt intermolecular associations, promoting their formation. Consistently, ζ-potential measurements show a narrower distribution for lignin treated at higher temperatures, indicating enhanced colloidal uniformity, despite a shift toward less negative values that remain below −30 mV (moderately stable colloids) (Supplementary Figure 3). The coexistence of highly stable yet very small lignin colloids plays a critical role in determining the porosity of the lignin filter cake and filter paper. These particles are close to or even below the average pore size in the filter cake and the filter membrane, which can impact filtration resistance and solid lignin recovery yield. Within the conditions examined, thermal treatment at 85 °C represents an optimal balance, achieving the highest lignin yield while maintaining the lowest filtration resistance. Future studies should systematically investigate additional parameters, such as pH, ionic strength, and time, to better control the formation of these small colloidal particles during the low pH washing step in the LignoBoost process. Such a control may enable further increases in lignin yield without compromising filtration efficiency.

3.4. Effects of the Heating Process on the Lignin Chemical Structure, Radicals, and Molar Mass

The above results show the physical changes (particle size and distribution) resulting from thermal treatment, which can alter lignin filter cake porosity and affect the volumetric flow rate. Additionally, lignin has highly reactive functional groups (phenols and unsaturated bonds) and temperature-sensitive linkages that readily react, leading to irreversible changes. Semiquantitative ^{13}C nuclear magnetic resonance (NMR) is used to characterize the linkages and functional groups.[25] Specifically, filtrated lignin A before and after acetylation was analyzed (Supplementary Figures 4 and 5). Acetylation with acetic anhydride can functionalize surface hydroxyl groups with acetyl groups, enabling characterization of linkages, such as the degree of condensation, identification of guaiacol units, and tagging different types of hydroxyl groups (175−168 ppm). Supplementary Table 3 provides more details about the calculation.

Our results show that linkages such as β-O-4, β-β, and β-5 do not show apparent differences or trends with changing temperature. Similarly, the functional groups, especially methoxy groups and total hydroxyl groups, including aliphatic hydroxyl and aromatic hydroxyl groups, have a variance of less than 2%, suggesting the chemical resilience of lignin under thermal treatment. On the other hand, there have been apparent decreases in ester linkages and aromatic hydrogen (ArH) that exceed their relative standard deviations (RSDs). This can be attributed to the hydrolysis of the ester bond under acidic conditions and newly formed condensed reactions during the treatment.

Temperature-sensitive radicals are also present in lignin suspension that can be characterized by electron paramagnetic resonance (EPR). The first-derivative EPR spectra recorded at X-band frequencies display a characteristic signal with a g-value of 2.0016 (Figure 5a). The g-value is a fundamental parameter that quantifies the interaction between an unpaired electron and an external magnetic field. It serves as a fingerprint to identify and characterize different paramagnetic species, indicating the presence of stable organic radicals (with a free-electron g-value of 2.00231). The spectral line shape remains unchanged for lignin treated at different temperatures,

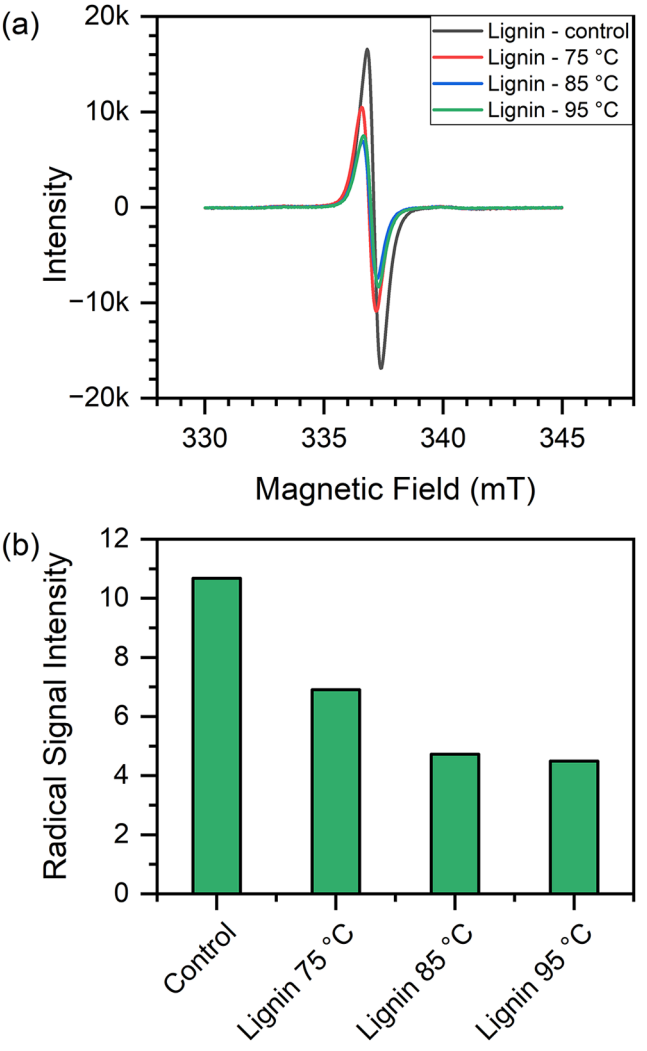

Figure 5. Characterization of stable radicals in filtrated lignin A based on the electron paramagnetic resonance: (a) the first derivative EPR spectra and (b) radical signal concentration.

suggesting that the radical species are similar. After thermal treatment, the overall radical signal intensity diminishes. Compared with the control group, the quantitative analysis of radical intensity reveals significant reductions of 35% at 75 °C, 56% at 85 °C, and 58% at 95 °C (Figure 5b). EPR data indicate that heating lignin suspension can promote radical cross-linking reactions in an acidic aqueous solution so that the radical concentration in the extracted lignin is becoming lower. The associated area.

Our DSC results show a considerable amount of heat released at 75−100 °C (Supplementary Figure 6), indicating an exothermic reaction that may relate to radical cross-linking. The exothermic peak is smaller after lignin thermal treatment, especially at 75 and 95 °C. This may be attributed to a decrease in radical concentration, leading to fewer radical-mediated covalent reactions. Continuously heating lignin to 120 °C can soften it (a higher molar mass fraction) until around 180 °C. Then, cooling down the lignin from 200 to 20 °C shows a similar glass transition temperature (T_g = 157 °C) under different heat treatments. We then heat the lignin again, showing the glass transition without any exothermic process, and T_g remains stable under different treatment temperatures.

https://doi.org/10.1021/acssuschemeng.5c12647
ACS Sustainable Chem. Eng. XXXX, XXX, XXX−XXX

Changes in chemical structure and radical composition can change the molar mass of the lignin macromolecule.[26] Gel permeation chromatography (GPC) is used to analyze the molecular weight traces (Figure 6). Increasing the treatment temperature slightly increases the molecular weight (Table 1), and molecular weight traces show a higher intensity in the high-molecular-weight region and a broader molecular weight distribution. These changes suggested the presence of slight, irreversible chemical changes as we heated the lignin in the acidic aqueous solution, consistent with the above chemical structure analysis.

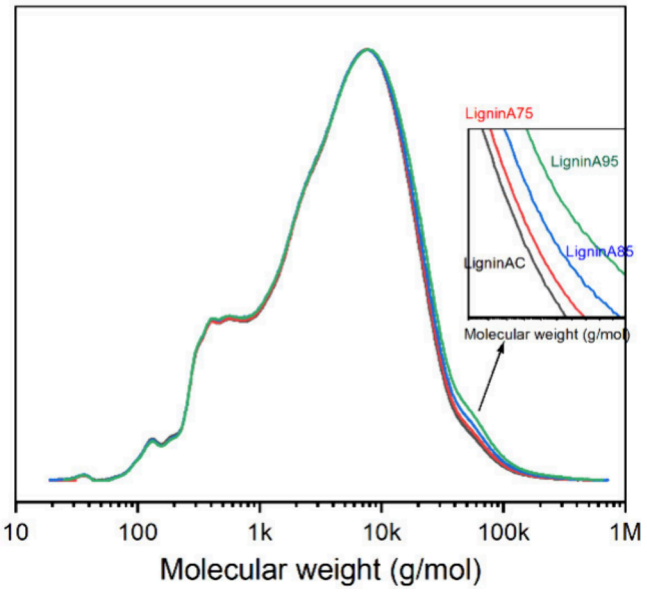

Figure 6. Molecular weight traces of lignin A under different conditions.

Table 1. Chemical Structure of Lignin after the Heating Treatment in Terms Functional Groups, Linkages, and Chemical Structures

	Lignin AC	Lignin A75	Lignin A85	Lignin A95
Glass transition temperature (T_g, °C)	157.2	156.5	156.0	158.5
Molecular weight				
M_w (g/mol)	9086	9376	9850	10738
M_n (g/mol)	1339	1347	1362	1422
Đ	6.79	6.96	7.23	7.55
Linkages (100 Ar)				
β-O-4	2.90	3.84	2.91	4.65
β-β	3.6	3.7	2.9	3.1
β-5	3.1	3.6	2.5	2.9
Degree of condensation	65.5	66.1	78.2	70.6
Total COOR	18.4	16.8	16.4	16.3
Functional groups (100 Ar)				
Total C═O	27.3	20.5	22.5	15.8
MeO	82.1	82.6	82.5	83.8
ArH	209.2	205.4	194.3	200.2
Total OH	119.2	117.5	117.8	120.0
Aliphatic OH	47.3	51.3	48.2	45.2
Primary AlOH	32.2	29.8	35.0	31.7
Secondary AlOH	15.1	14.4	15.6	15.0
Phenolic OH	74.3	71.7	69.6	74.8
5-free Phenolic OH	39.0	37.8	39.3	39.0
5-Sub Phenolic OH	32.9	35.4	30.5	34.6
Guaiacyl unit	74.7	71.5	72.5	70.8
Other composition (100Ar)				
Carbohydrates	2.81	1.50	2.67	2.45

3.5. Potential Driving Force for Particle Change during Heating Treatment

Overall, the driving force for changes in the lignin particle size during thermal treatment can be attributed to both physical and chemical mechanisms. Like normal colloids following the Derjaguin−Landau−Verwey−Overbeek (DLVO) theory, the stability of lignin colloids is governed by two competing forces: electrostatic repulsion and van der Waals attraction. Our studies show that temperature plays a crucial role in influencing these forces. Heating lignin at 55 °C decreases intermolecular interactions (van der Waals forces, hydrogen bonding, and $\pi-\pi$ interactions), facilitating the formation of submicron or micron lignin particles that are readily dispersed in aqueous acidic solutions.[27] The lower ζ-potential indicates the presence of enriched electrical double layers on the particle surfaces, which exerts a strong repulsion between lignin macromolecules.[28] Compared to larger particles, smaller particles have a higher surface area, which can easily lead to coalescence and Ostwald ripening while heating the lignin particles.[27]

An increase in the number of larger particles and a smaller PSD can improve the lignin cake porosity and reduce filter resistance, but this is not always the case in lignin filtration. The presence of smaller, stable lignin colloids in the system can both positively and negatively influence the overall process (Figure 7). On the one hand, larger porosity may allow smaller particles to pass through the lignin filter cake but block the filter paper, thereby decreasing filtration resistance. One piece of evidence is the lowest yield at 95 °C. If these smaller particles remain with the lignin cake, this can increase the lignin recovery yield but lower the filtration resistance (control group and 75 °C). As such, we need to optimize the conditions to find a good combination between the lignin yield and filtration efficiency. In this experiment, thermal treatment at 85 °C is the optimal condition.

Chemically, numerous surface functional groups and linkages are present in the lignin particles. Thermal treatment can initiate chemical reactions that irreversibly alter lignin structure, thereby negatively influencing its consistency (molar mass, hydroxyl groups, and T_g) as a raw material.[29] Table 1 shows an increasing degree of condensation and a decreasing number of carbonyl (C═O) groups for the thermally treated lignin. Our EPR results indicate that lignin contains stable radicals that decrease after the heating treatment, suggesting that these radicals may contribute to the formation of covalent radical bonds and other structural alterations associated with increasing molar mass. Also, the DSC curve indicates a weaker exothermic reaction for thermally treated lignin. One potential reaction involves phenol radicals in lignin, which can react with other radicals to form C−C linkages.[30] An acidic medium with an oxygen atmosphere can further promote chemical reactions, such as the condensation reaction between phenols and aldehydes. One piece of evidence is that the temperature window in the DSC curves is similar to the acidic-catalyzed phenol-form-

https://doi.org/10.1021/acssuschemeng.5c12647
ACS Sustainable Chem. Eng. XXXX, XXX, XXX−XXX

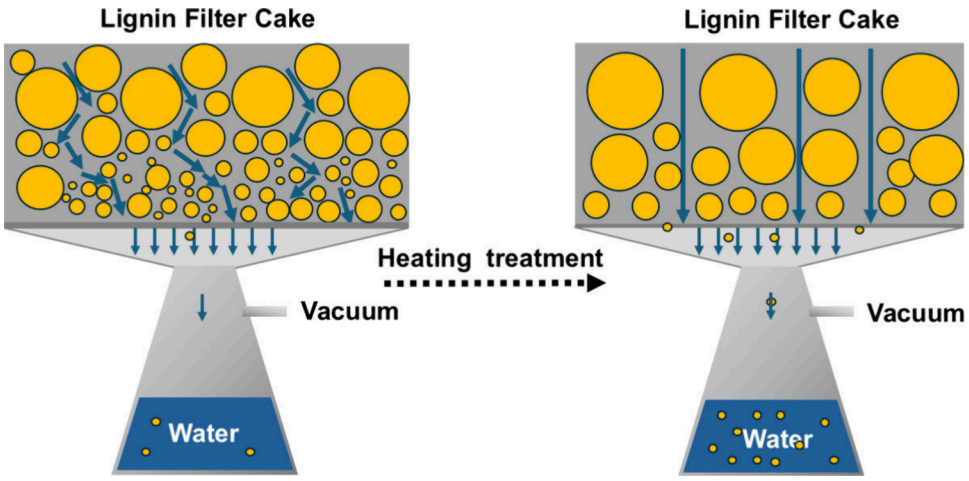

Figure 7. Scheme to explain the impacts of heating treatment on lignin cake formation and filtration efficiency.

aldehyde reaction.[31] There may also be the potential to hydrolyze the ester linkages in kraft lignin under these processing conditions. These types of reactions can have competence to influence the molar mass. These reactions are another factor driving particle size changes, which may need further investigation, for example, by lignin model studies, to understand them more fundamentally. Overall, our results (Table 1) show that changes in T_g, the abundance of functional groups, such as methoxy, aliphatic hydroxyl, and phenolic groups, and even molar mass are relatively minor, indicating that the heating treatment has only a slight effect on the consistency of the recovered.

4. CONCLUSION

In this study, we investigated the effect of heat treatment (75−95 °C) on the filtration volumetric flow rate during the low-pH washing step of the LignoBoost process. Heating treatment increased the lignin particle size and reduced the number of smaller lignin particles. These changes altered the porosity of the lignin filter cake, resulting in lower filtration resistance and a higher volumetric flow rate, albeit at the expense of a reduced solid yield. In addition to physical mechanisms, such as Ostwald ripening, chemical changes also occurred, including radical-induced condensation and ester hydrolysis, which led to an increase in molar mass. Despite these changes, key properties, including the total hydroxyl group content and glass transition temperature, remained largely unaffected across the investigated temperature range. Overall, this work provides valuable insights into the interective effects of the lignin structure and recovery conditions, which are critical for the efficient large-scale valorization of kraft lignin.

■ ASSOCIATED CONTENT

Supporting Information

The Supporting Information is available free of charge at https://pubs.acs.org/doi/10.1021/acssuschemeng.5c12647.

Supplementary figures including the sedimentation of lignin particles in the DLS cuvette, ζ-potential under different conditions (control, 75 °C, 85 °C, and 95 °C), NMR spectra for lignin and acetylated lignin, and DSC curves; supplementary table showing the volume weighted and number weighted particle size calculation based on Mastersizer; and ^{13}C NMR peak assignment and calculation (PDF)

■ AUTHOR INFORMATION

Corresponding Author

Li-Yang Liu − *Department of Chemistry and Chemical Engineering, Chalmers University of Technology, SE-412 96 Gothenburg, Sweden; Wallenberg Wood Science Center, Department of Chemistry and Chemical Engineering, Chalmers University of Technology, SE-412 96 Gothenburg, Sweden;* orcid.org/0000-0003-1868-6680; Email: liyang.liu@chalmers.se

Authors

Hampus Johansson − *Department of Chemistry and Chemical Engineering, Chalmers University of Technology, SE-412 96 Gothenburg, Sweden*

Liam Mistry − *Department of Chemistry and Chemical Engineering, Chalmers University of Technology, SE-412 96 Gothenburg, Sweden; Wallenberg Wood Science Center, Department of Chemistry and Chemical Engineering, Chalmers University of Technology, SE-412 96 Gothenburg, Sweden*

Ahilan Manisekaran − *Department of Chemistry and Chemical Engineering, Chalmers University of Technology, SE-412 96 Gothenburg, Sweden; Wallenberg Wood Science Center, Department of Chemistry and Chemical Engineering, Chalmers University of Technology, SE-412 96 Gothenburg, Sweden*

Henrik Sarge − *Department of Chemistry and Chemical Engineering, Chalmers University of Technology, SE-412 96 Gothenburg, Sweden*

Anette Larsson − *Department of Chemistry and Chemical Engineering, Chalmers University of Technology, SE-412 96 Gothenburg, Sweden; Wallenberg Wood Science Center, Department of Chemistry and Chemical Engineering, Chalmers University of Technology, SE-412 96 Gothenburg, Sweden;* orcid.org/0000-0002-6119-8423

Merima Hasani − *Department of Chemistry and Chemical Engineering, Chalmers University of Technology, SE-412 96 Gothenburg, Sweden; Wallenberg Wood Science Center, Department of Chemistry and Chemical Engineering,*

Chalmers University of Technology, SE-412 96 Gothenburg, Sweden

Hans Theliander − *Department of Chemistry and Chemical Engineering, Chalmers University of Technology, SE-412 96 Gothenburg, Sweden; Wallenberg Wood Science Center, Department of Chemistry and Chemical Engineering, Chalmers University of Technology, SE-412 96 Gothenburg, Sweden;* orcid.org/0000-0002-2120-6513

Complete contact information is available at: https://pubs.acs.org/10.1021/acssuschemeng.5c12647

Notes

The authors declare no competing financial interest.

■ ACKNOWLEDGMENTS

We thank Hanna Karlsson (Valmet), Anders Littorin (Valmet), and Rickard Wadsborn (Stora Enso) for their technical support and lignin supply. We also acknowledge Ulrika Brath (Swedish NMR Center) and Shuichi Haraguchi, Linus Kron, and Carolina Marion de Godoy (Chalmers) for assistance with DSC, GPC, and UV analyses. This work was supported by the Wallenberg Wood Science Center (WWSC 3.0: KAW 2021.0313).

■ REFERENCES

(1) Argyropoulos, D. D. S.; Crestini, C.; Dahlstrand, C.; Furusjo, E.; Gioia, C.; Jedvert, K.; Henriksson, G.; Hulteberg, C.; Lawoko, M.; Pierrou, C.; et al. Kraft Lignin: A Valuable, Sustainable Resource, Opportunities and Challenges. *ChemSusChem* **2023**, *16* (23), No. e202300492.

(2) Chakar, F. S.; Ragauskas, A. J. Review of current and future softwood kraft lignin process chemistry. *Industrial Crops and Products* **2004**, *20* (2), 131−141.

(3) Gellerstedt, G. Softwood kraft lignin: Raw material for the future. *Industrial Crops and Products* **2015**, *77*, 845−854.

(4) De Saegher, T.; Deroma, M.; Atanasova, B.; Van Geem, K. M.; De Clercq, J.; Lauwaert, J.; Verberckmoes, A. Maximizing the valorization potential of lignin through optimization of the Soda pulping conditions. *Sep. Purif. Technol.* **2025**, *354*, 128900.

(5) Liu, L.-Y.; Karaaslan, M. A.; Hua, Q.; Cho, M.; Chen, S.; Renneckar, S. Thermo-Responsive Shape-Memory Polyurethane Foams from Renewable Lignin Resources with Tunable Structures-Properties and Enhanced Temperature Resistance. *Ind. Eng. Chem. Res.* **2021**, *60* (32), 11882−11892.

(6) Hua, Q.; Liu, L. Y.; Karaaslan, M. A.; Renneckar, S. Aqueous Dispersions of Esterified Lignin Particles for Hydrophobic Coatings. *Front. Chem.* **2019**, *7*, 51501−51510.

(7) Karaaslan, M. A.; Lin, L.-T.; Ko, F.; Renneckar, S. Carbon Aerogels From Softwood Kraft Lignin for High Performance Supercapacitor Electrodes. *Frontiers in Materials* **2022**, DOI: 10.3389/fmats.2022.894061.

(8) Li, Q.; Li, M.; Lin, H. S.; Hu, C.; Truong, P.; Zhang, T.; Sue, H. J.; Pu, Y.; Ragauskas, A. J.; Yuan, J. S. Non-Solvent Fractionation of Lignin Enhances Carbon Fiber Performance. *ChemSusChem* **2019**, *12* (14), 3249−3256.

(9) Wan, X.; Liu, L.-Y.; Karaaslan, M. A.; Hua, Q.; Shen, F.; Sipponen, M.; Renneckar, S. Circular poly(ethylene terephthalate) with lignin-based toughening additives. *Chemical Engineering Journal* **2025**, *504*, 158255.

(10) Bessler, K. The characterization of acetone fractionated and unfractionated, chemically modified lignin-ecoflex thermoplastic blend. Thesis, The University of British Columbia, Vancouver, 2021, DOI: 10.14288/1.0398121.

(11) Andersson, M.; Pylypchuk, I. V.; Alexakis, A. E.; Liu, L. Y.; Sipponen, M. H. Esterified Lignin Nanoparticles for Targeted Chemical Delivery in Plant Protection. *ACS Appl. Mater. Interfaces* **2025**, *17* (1), 1931−1941.

(12) Tomlinson, G. H. Method of Treating Lignocellulosic Material. US2406867A, US, 1946.

(13) Hu, Z.; Du, X.; Liu, J.; Chang, H.-m.; Jameel, H. Structural Characterization of Pine Kraft lignin: BioChoice lignin vs Indulin AT. *J. Wood Chem. Technol.* **2016**, *36* (6), 432−446.

(14) Zhu, W.; Westman, G.; Theliander, H. Investigation and Characterization of Lignin Precipitation in the LignoBoost Process. *J. Wood Chem. Technol.* **2014**, *34* (2), 77−97.

(15) Tomani, P. The lignoboost process. *Cellul. Chem. Technol.* **2010**, *44* (1−3), 53−58.

(16) Öhman, F. Precipitation and separation of lignin from kraft black liquor. Thesis, Chalmers University of Technology, Gothenburg, 2002.

(17) Wallmo, H.; Littorin, A. Methods and Systems for producing lignin. EP4363661A1, Sweden, 2022.

(18) Sewring, T. Precipitation of kraft lignin from Aqueous Solutions. Thesis, Chalmers University of Technology, 2019.

(19) Wallmo, H. Lignin extraction from black liquor: precipitation, filtration, and washing. Thesis, Chalmers University of Technology, Gothenburg, 2008.

(20) Manisekaran, A.; Grysan, P.; Duez, B.; Schmidt, D. F.; Lenoble, D.; Thomann, J. S. Solvents drive self-assembly mechanisms and inherent properties of Kraft lignin nanoparticles (<50 nm). *J. Colloid Interface Sci.* **2022**, *626*, 178−192.

(21) Henrik-Klemens, Å.; Caputo, F.; Ghaffari, R.; Westman, G.; Edlund, U.; Olsson, L.; Larsson, A. The glass transition temperature of isolated native, residual, and technical lignin. *Holzforschung* **2024**, *78* (4), 216−230.

(22) Kron, L.; Hasani, M.; Theliander, H. Heterogenous Diffusion and Reaction Model of Kraft Delignification at the Cell Wall Level. *Ind. Eng. Chem. Res.* **2025**, *64* (3), 1497−1507.

(23) Liu, L.-Y.; Cho, M.; Sathitsuksanoh, N.; Chowdhury, S.; Renneckar, S. Uniform Chemical Functionality of Technical Lignin Using Ethylene Carbonate for Hydroxyethylation and Subsequent Greener Esterification. *ACS Sustain. Chem. Eng.* **2018**, *6* (9), 12251−12260.

(24) Wakeman, R. The influence of particle properties on filtration. *Sep. Purif. Technol.* **2007**, *58* (2), 234−241.

(25) Balakshin, M.; Capanema, E. Comprehensive Structural Analysis of Biorefinery Lignins with a Quantitative 13C NMR Approach. *RSC Adv.* **2015**, *5* (106), 87187−87199.

(26) Liu, L.-Y.; Chen, S.; Ji, L.; Jang, S.-K.; Renneckar, S. One-pot route to convert technical lignin into versatile lignin esters for tailored bioplastics and sustainable materials. *Green Chem.* **2021**, *23* (12), 4567−4579.

(27) Yin, Y.; Wu, J.; Qin, S.; Tang, A.; Li, Q.; Liao, D.; Tang, Y.; Liu, Y. Study on Thermally Induced Lignin Aggregation Kinetics for the Preparation of Uniformly Sized Lignin Nanoparticles in Water. *Langmuir: the ACS journal of surfaces and colloids* **2024**, *40* (40), 21152−21160.

(28) Li, Q.; Zhang, H.; Lee, J.; Wan, C. Size-tailorable lignin nanoparticle synthesis: effects of solution chemistry and DLVO forces on amphiphilic balance of lignin. *Green Chem.* **2023**, *25* (22), 9301−9312.

(29) Constant, S.; Wienk, H. L. J.; Frissen, A. E.; Peinder, P. d.; Boelens, R.; van Es, D. S.; Grisel, R. J. H.; Weckhuysen, B. M.; Huijgen, W. J. J.; Gosselink, R. J. A.; et al. New Insights into the Structure and Composition of Technical Lignins: a Comparative Characterisation Study. *Green Chem.* **2016**, *18* (9), 2651−2665.

(30) Cui, C.; Sadeghifar, H.; Sen, S.; Argyropoulos, D. S. Toward Thermoplastic Lignin Polymers; Part II: Thermal & Polymer Characteristics of Kraft Lignin & Derivatives. *BioResources* **2012**, *8* (1), 864−886.

(31) Lu, K. T.; Luo, K. M.; Lin, S. H.; Su, S. H.; Hu, K. H. The Acid-Catalyzed Phenol-Formaldehyde Reaction. *Process Safety and Environmental Protection* **2004**, *82* (1), 37−47.